Electronic mechanism for toughness enhancement in $Ti_xM_{1-x}N$ (M=Mo and W)

Davide Sangiovanni, Valeriu Chirita and Lars Hultman

Original Publication:

Davide Sangiovanni, Valeriu Chirita and Lars Hultman, Electronic mechanism for toughness enhancement in TixM1-xN (M=Mo and W), 2010, PHYSICAL REVIEW B, (81), 10, 104107.
http://dx.doi.org/10.1103/PhysRevB.81.104107

Electronic mechanism for toughness enhancement in $Ti_xM_{1-x}N$ (M=Mo and W)

D. G. Sangiovanni, V. Chirita, and L. Hultman
Thin Film Physics, Department of Physics, Chemistry and Biology (IFM), Linköping University, SE-581 83 Linköping, Sweden
(Received 9 December 2009; revised manuscript received 4 February 2010; published 15 March 2010)

Toughness, besides hardness, is one of the most important properties of wear-resistant coatings. We use *ab initio* density-functional theory calculations to investigate the mechanical properties of ternary metal nitrides $Ti_xM_{1-x}N$, with M=Mo and W, for x=0.5. Results show that Mo and W alloying significantly enhances the toughness of TiN. The electronic mechanism responsible for this improvement, as revealed by electronic structure calculations, stems from the changes in charge density induced by the additional transition-metal atom. This leads to the formation of a layered electronic arrangement, characterized by strong, respectively, weak, directional bonding, which enables a selective response to strain, respectively, shear, deformations of the structures and yields up to 60% decrease in C_{44} values.

DOI: 10.1103/PhysRevB.81.104107 PACS number(s): 81.05.Je, 68.60.Bs, 71.15.Mb

I. INTRODUCTION

Within the last decades, a vast amount of experimental and theoretical studies has been devoted to the study of transition-metal nitride thin films. Among these, TiN ranks as one of the most widely explored system due to its excellent performance as hard, wear- and corrosion-resistant coating.[1] An equally impressive scientific effort has been committed to TiN-based ternaries, primarily TiAlN, as the additional transition metals offer increased possibilities for fine-tuning mechanical and/or electrical properties by adjusting metal ratios.[2,3] For the same reasons, in recent years, quaternary compounds have received increasing attention in order to surpass the properties of TiAlN. Thus, yttrium was shown to enhance oxidation resistance and hardness,[4] TiAlZrN has been found to have excellent adhesive strength to the substrate in terms of critical load,[5] TiAlCrN and TiAlHfN have higher wear resistance and hardness,[6–8] while TiAlVN has been introduced as possible candidate for low-friction coatings due to its enhanced tribological properties.[9] Generally, for all these compounds, results show that as long as the B1-NaCl structure is maintained, one can achieve these goals.

To achieve hardening as a desired property in the nitrides, the structure and bonding should be designed to hinder dislocation motion during mechanical deformations. However, hard materials are less responsive to plastic deformations, which may result in brittle fracture due to crack initiation and/or propagation,[10] thus reducing their potential use. The ability of a material to withstand plastic deformation before fracturing is called toughness. Evidently, in the design of novel coatings, high hardness and toughness represents a highly sought after combination of properties, particularly for enhancing the wear resistance of transition-metal nitride coatings.

Material toughness depends strongly, if not exclusively, on its ductility or its ability to deform plastically. Pugh, who analyzed plastic flow and brittle fracture in metals,[11] found an empirical relationship connecting these processes to the shear and bulk moduli of the metal. According to his formulation, low G/B values, i.e., <0.5, are associated with malleability, while higher values indicate brittleness. The brittle-ductile behavior for a number of cubic materials was quantified by Pettifor,[12] who related the Cauchy pressure $C_{12}-C_{44}$, to the angular character of bonds. Based on his findings, positive Cauchy pressures correspond to a metallic character in bonds and to a ductile behavior of the material. For metal nitrides, it was also shown that their hardness is proportional to their bulk or shear modulus.[13] Herein, we use these physical criteria to estimate hardness and ductility in all considered compounds.

The aim of this work is to rigorously explore the possibility of increasing toughness, while retaining hardness, in transition-metal nitrides. Several attempts have been made in recent years in this direction. In a preliminary theoretical study,[14] Mo and W have been identified, among other transition metals, as the best candidates for improving the ductility of TiN upon alloying with 25% Mo, respectively, W. Based on these results, Zhao *et al.*[15] mapped the hardness and ductility trend for a number of binary and ternary metal nitrides and identified a number of potential ternary combinations, which might achieve this goal. An alternative approach was presented by Hugosson *et al.*,[16] who employed valence electron-density tuning of $Nb_xZr_{1-x}N$ systems to set the cubic-B1 and wurtzite structures to equal energies, thus promoting the formation of stacking faults during crystal growth with respect to either structures. This was shown to increase hardness by hindering dislocation slip across the stacking faults,[17] while ductility in principle would be promoted along the faults by virtue of mechanically induced faulting or (de)twinning.

In this paper, we report the results of our *ab initio* investigations of the mechanical properties and electronic structure of ternary transition-metal nitrides $Ti_xM_{1-x}N$, where M=Mo and W, for x=0.5. This choice is based on the fact that these ternaries have been successfully synthesized in the laboratory for metal concentrations of up to 60%,[18–21] thus offering a solid reference point for our calculations. We carry out density-functional theory (DFT) calculations to accurately calculate key elastic properties of these compounds and compare them to those of two well-known hard coating materials: TiN and $Ti_{0.5}Al_{0.5}N$. Our results show that these ternaries exhibit small changes in Young moduli, significantly higher bulk moduli (up to 16%), and substantially lower C_{44} values (up to 60%), compared to pure TiN and

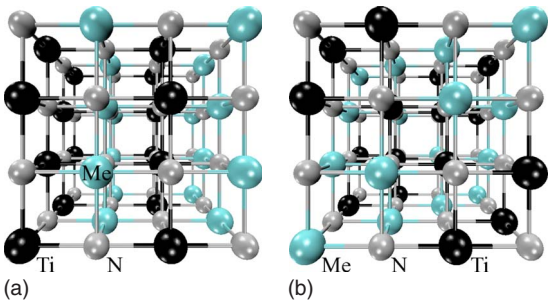

FIG. 1. (Color online) 64-atom supercells used in VASP calculations: (a) C#1 configuration with maximum number of *M*-Ti bonds; (b) C#3 configuration with minimum number of *M*-Ti bonds.

$Ti_{0.5}Al_{0.5}N$. These results suggest a substantial increase in the toughness of these compounds, as they have comparable hardness with the pure binary or ternary, but are considerably more ductile. We investigate the electronic structure of these compounds and find that the addition of Mo or W induces significant changes in the charge density of the original binary. Our analysis demonstrates that upon deformation, a layered electronic arrangement is induced in the ternaries, which enables a selective response of the B1 structure to strain, respectively, shear, and explains the dual hard-ductile behavior of these novel compounds.

II. METHODOLOGY

The DFT calculations reported herein are performed with the Vienna ab initio simulation package (VASP) (Ref. 22) in the generalized gradient approximation of Perdew-Wang (GGA-PW91).[23] In all our systems, electron-ion interactions are described by the projector augmented wave (PAW) potentials[24] and the energy is minimized using a large energy cutoff of 500 eV for the plane-wave basis to achieve total-energy convergence within 10^{-5} eV. This high-accuracy level is maintained in our structure relaxations and density of states (DOS) calculations by using $4\times4\times4$, respectively, $16\times16\times16$, **k**-point grids to sample the Brillouin zone with the Monkhorst-Pack (MP) scheme.[25]

The atomic configurations used in our investigations contain in all cases 64 atoms, as shown in Fig. 1. We note that for ternaries in the B1 structure, one can obtain different, nonequivalent configurations based on the actual arrangement of atoms in the metallic sublattice.[26] The two extreme situations are obtained if one considers the maximum Fig. 1(a), respectively, minimum Fig. 1(b), number of Ti-*M* bonds, denoted as C#1, respectively, C#3, in the original paper.[27] We carry out energy minimization calculations to determine the equilibrium volume of $Ti_{0.5}Mo_{0.5}N$ and $Ti_{0.5}W_{0.5}N$ for the C#1 and C#3 configurations and in both cases, we find that the C#3 configuration is energetically favored (see Table I). We also find, for both ternaries (Table I), the C#3 configuration as more stable in terms of energy of formation, calculated as

$$E_f = E_{Ti_{0.5}M_{0.5}N} - 0.5E_{TiN} - 0.5E_{cubic/hexagonal(MN)}. \quad (1)$$

These results are in agreement with previous findings for $Ti_xAl_{1-x}N$,[27] showing the C#3 arrangement as the most stable configuration for concentrations of Al up to 74%. In fact, the C#3 configuration is characterized by alternating Ti-rich and W-rich $(1\bar{1}1)$ planes and corresponds to the CuPt-type atomic ordering observed experimentally for $Ti_xW_{1-x}N$ thin films.[19] Consequently, we present herein only the results for the C#3 configuration. Our energy of formation estimations, according to which the B1 structure is energetically favored with respect to the separate cubic binaries, are nevertheless confirmed by the experimental studies showing that $Ti_xW_{1-x}N$ (Refs. 18 and 19) and $Ti_xMo_{1-x}N$ (Refs. 20 and 21) thin films, with $0\leq x\leq0.6$, can be synthesized in the B1-NaCl structure. Phase transformation by spinodal decomposition in the cubic state or nucleation and growth can be expected at higher concentrations, as suggested by the energy of formation results we report for the hexagonal binaries (Table I).

We calculate for both configurations lattice constants *a*, bulk moduli *B*, elastic constants C_{11}, C_{12}, and C_{44}, Young moduli *E*, shear moduli *G*, and Poisson's ratios ν. Ideal lattice constants are found by minimizing the total energy for different lattice parameters and the bulk modulus is evaluated by fitting the total energy-volume curve to the Birch-Murnaghan equation of state.[28] For cubic systems, the complete set of elastic constants is obtained by determining C_{11}, C_{12}, and C_{44}. To calculate C_{11} and C_{12}, a sufficiently small tetragonal distortion δ is applied to the cubic cell while keeping the cell volume constant. The strain tensor ε corresponding to this tetragonal distortion is then given by

$$\varepsilon = \begin{pmatrix} +\delta/2 & 0 & 0 \\ 0 & +\delta/2 & 0 \\ 0 & 0 & -\delta \end{pmatrix} \quad (2)$$

and the associated strain energy density, $U_{tetr}(\delta)$, is defined by

TABLE I. Total energies (E_{tot}) and energies of formation (E_f) for $Ti_{0.5}Mo_{0.5}N$ and $Ti_{0.5}W_{0.5}N$ in the C#1 and C#3 configurations.

	Configuration	E_{tot} (eV/atom)	E_f vs cub (*M*N) (eV/atom)	E_f vs hex (*M*N) (eV/atom)
$Ti_{0.5}W_{0.5}N$	C#1	−10.1405	−0.0774	0.1281
	C#3	−10.1626	−0.0994	0.1060
$Ti_{0.5}Mo_{0.5}N$	C#1	−9.7364	−0.0299	0.1298
	C#3	−9.7618	−0.0554	0.1043

TABLE II. Comparison of DFT results with experimental values for TiN and $Ti_{0.5}Al_{0.5}N$.

	Present work	*Ab initio* calculations	Experiments
TiN			
a (Å)	4.254	4.260[a], 4.221[b], 4.246[c], 4.255[d], 4.240[e]	4.240[g], 4.240[h]
B (GPa)	290	295[a], 270[b], 287[c], 276[d], 292[e]	318[f], 303[g], 346[h], 237[i]
E (GPa)	489	514[a], 487[b], 456[c], 414[d], 539[e]	475[f], 510[g], 455[h], 429[i]
G (GPa)	200	213[a], 203[b], 189[c], 226[e]	190[f], 209[g], 178[h], 179[i]
C_{44} (GPa)	159	166[a], 168[b], 165[c], 154[d], 172[e]	163[f], 156[h], 168[i]
C_{11} (GPa)	640	671[a], 610[b], 585[c], 615[e]	625[f], 626[h], 498[i]
C_{12} (GPa)	115	106[a], 100[b], 137[c], 131[e]	165[f], 206[h], 106[i]
ν	0.219	0.209[a], 0.199[b], 0.235[c], 0.192[e]	0.251[f], 0.219[g], 0.281[h], 0.198[i]
$Ti_{0.5}Al_{0.5}N$			
a (Å)	4.175	4.175[d], 4.195[k], 4.184[l]	4.178[l], 4.187[n], 4.173[m]
B (GPa)	269	260[d], 256[j], 258[k]	
E (GPa)	440	389[d], 454[j], 474[k]	438[l], 493[m]
G (GPa)	179	189[j], 199[k]	
C_{44} (GPa)	189	210[d], 185[j], 228[k]	
C_{11} (GPa)	488	515[j], 465[k]	
C_{12} (GPa)	159	127[j], 155[k]	
ν	0.227	0.204[j], 0.193[k]	

[a]Reference 14.
[b]Reference 35.
[c]Reference 34.
[d]Reference 27.
[e]Reference 33.
[f]Reference 29.
[g]Reference 30.
[h]Reference 31.
[i]Reference 32.
[j]Reference 36.
[k]Reference 37.
[l]Reference 4.
[m]Reference 38.
[n]Reference 39.

$$U_{tetr} = \frac{3}{4}\delta^2(C_{11} - C_{12}), \tag{3}$$

where U_{tetr} is obtained directly from VASP calculations using different values of δ. To obtain accurate results, we use distortions of less than 1%, i.e., $|\delta| \leq 0.01$, and estimate $C_{11}-C_{12}$ by least-squares fitting. We then use the relationship between bulk modulus and elastic constants,

$$B = \frac{C_{11} + 2C_{12}}{3}, \tag{4}$$

to calculate C_{11} and C_{12} according to

$$C_{11} = B + \frac{2}{3}(C_{11} - C_{12}), \tag{5}$$

$$C_{12} = B - \frac{1}{3}(C_{11} - C_{12}). \tag{6}$$

In similar fashion, we determine the C_{44} elastic constant by applying a small trigonal deformation (δ) and keeping the cell volume constant. In this case, the strain tensor ε and related trigonal strain energy are given by

$$\varepsilon = \begin{pmatrix} 0 & \delta & 0 \\ \delta & 0 & 0 \\ 0 & 0 & 0 \end{pmatrix}, \tag{7}$$

respectively,

$$U_{tri} = 2\delta^2 C_{44}. \tag{8}$$

Accurate estimations of U_{tri} are obtained directly from VASP calculations using sufficiently small distortions ($|\delta| \leq 0.01$) and C_{44} is determined by least-squares fitting. Finally, the shear modulus, Young's modulus, and Poisson's ratio are obtained from the following relations:

$$G = \frac{3C_{44} + C_{11} - C_{12}}{5}, \tag{9}$$

$$E = \frac{9BG}{3B + G}, \tag{10}$$

$$\nu = \frac{1}{2}\left(1 - \frac{E}{3B}\right). \tag{11}$$

III. RESULTS

In Table II, we present the results of our calculations for

TABLE III. Elastic properties of the two ternaries predicted in this work.

	a (Å)	B (GPa)	E (GPa)	G (GPa)	C_{44} (GPa)	C_{11} (GPa)	C_{12} (GPa)	$C_{12}-C_{44}$ (GPa)	G/B	ν
TiN	4.254	290	489	200	159	640	115	−44	0.690	0.219
$Ti_{0.5}Al_{0.5}N$	4.175	269	440	179	189	488	159	−30	0.665	0.227
$Ti_{0.5}Mo_{0.5}N$	4.300	321	382	147	77	655	153	76	0.458	0.302
$Ti_{0.5}W_{0.5}N$	4.298	336	394	151	60	720	145	85	0.449	0.305

TiN and $Ti_{0.5}Al_{0.5}N$. These are compared to the values reported in previous theoretical and experimental studies of the same compounds. We note that for TiN, our results are generally in excellent agreement with the experimental values reported for all the properties of interest herein.[29–32] With few exceptions, our results also compare extremely well to those obtained in similar DFT investigations.[14,27,33–35] The obvious differences between the sets of DFT values shown in Table II are typically expected and they are most probably due to variations in the LDA-GGA, or $\boldsymbol{k}$ point sampling, schemes used in each calculation. With respect to $Ti_{0.5}Al_{0.5}N$, we note that for bulk modulus, shear modulus, and the elastic constants, the reported values in the literature are primarily theoretical,[4,27,36,37] closely matching the results reported herein. Nevertheless, our calculations for lattice constant and Young modulus are in excellent agreement with the results of previous DFT investigations[4,27,36,37] and recently reported experimental values.[4,38,39]

The results of our calculations for the ternaries containing Mo and W are presented in Table III. As it can be seen, the 50% addition of Mo, respectively, W, in TiN has the effect of increasing the value of the lattice constant, from 4.25 to 4.30 Å, in both compounds. We find no experimental data for TiMoN while for TiWN, the reported value is ~4.25 Å.[18,19] This discrepancy can be explained as a combination of the typical, inherent LDA-GGA lattice overestimation and the difference between the nonideal CuPt ordering present in our C#3 configuration and that in the actual experiment. More significant, however, is the effect that these additions have on the bulk modulus, Young modulus, shear modulus, and the C_{44} elastic constant of TiN. Thus, bulk modulus increases by up to 16%, while for the Young and shear moduli, the values reported herein are somewhat lower compared to TiN and TiAlN. As mentioned before, the generally accepted rule is to associate hard compounds with high bulk, Young, and shear moduli values.[13] In fact, the Young modulus value reported here for $Ti_{0.5}Mo_{0.5}N$ (382 GPa) is in excellent agreement with the experimental value obtained in nanoindentation tests for $Ti_{0.52}Mo_{0.48}N$ (344 ± 11 GPa).[21] Importantly, in this work, Mo alloying is found to enhance TiN hardness for most Mo concentrations. Clearly, corroborated with this experiment, our results confirm that the ternaries obtained by alloying TiN with Mo and W have a hardness which, if not greater, is at least comparable to that of both TiN and TiAlN.

Even more noteworthy, however, is the effect that the addition of Mo or W in TiN has on the other property monitored herein, namely, the drastic decrease by up to 62%, in C_{44} values. These changes translate into significant shifts in the Poisson ratio, Cauchy pressure, and G/B ratio, thus affecting the ductility of these ternaries. In Fig. 2, we use the Pugh and Pettifor criteria mentioned above to map the brittle and/or ductile trend/behavior of all the compounds studied herein. As it can be seen, the addition of Mo and W induces a decisively ductile character in the clearly brittle TiN and TiAlN. Remarkably, this change can be achieved without significant losses in terms of hardness.

In order to understand the origin of such supertoughening in TiMoN and TiWN, we analyze the electronic structure of these ternaries and monitor the modifications induced by the additional transition-metal atoms in the compound charge densities and density of states. In Fig. 3, we plot the (001) charge-density maps of the four compounds for the relaxed structures at the equilibrium volume. As it can be seen [Fig. 3(a)] in TiN, the Ti-N bonds have a strong ionic character (note the high concentration of electrons surrounding the nuclei), as well as a covalent nature, due to the bonding (σ) d(Ti)-p(N) orbital interaction. As expected, $Ti_{0.5}Al_{0.5}N$ [Fig. 3(b)] exhibits enhanced directional bonding compared to TiN due to the additional p-p orbital interactions between Al and N atoms. By contrast, the presence of Mo or W clearly delocalizes more charge in the regions between the nuclei [Figs. 3(c) and 3(d)], translating into a significantly more pronounced covalent character of the Mo-N or W-N bonds in these compounds. It is also interesting to remark that in these ternaries, the electrons surrounding Mo or W have a tendency to spread toward second-nearest neighbors.

To clarify the role played by the observed charge delocalization in the vicinity of the Mo or W nuclei, we examine the

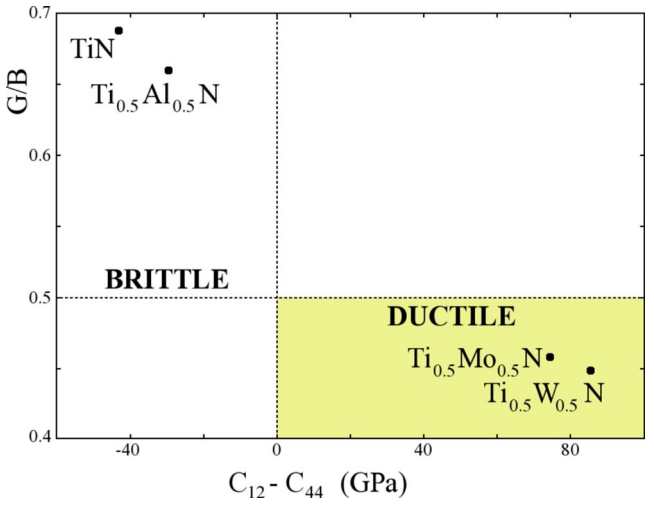

FIG. 2. (Color online) Map of brittleness and ductility trends of the compounds as estimated in this work.

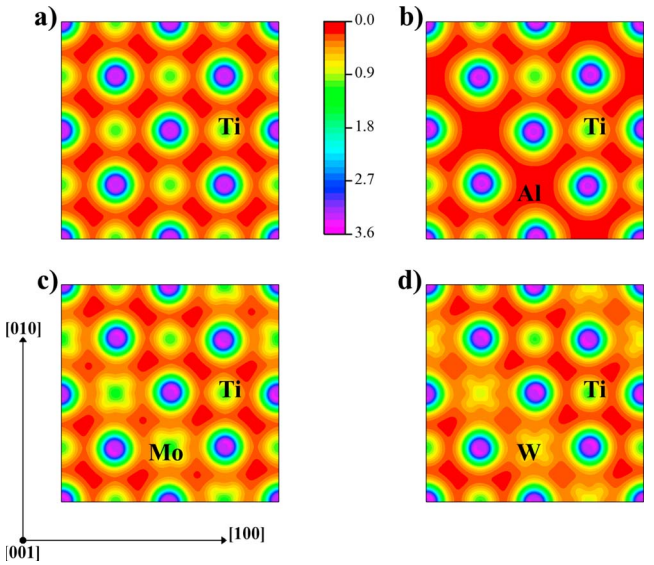

FIG. 3. (Color online) Charge densities of relaxed structures. Color scale units are electrons/Å^3: (a) TiN, (b) TiAlN, (c) TiMoN, and (d) TiWN.

changes induced by tetragonal, respectively, trigonal, deformations in the charge density of these compounds. The overall effects are illustrated in Fig. 4, where we plot the charge-density maps of structures subjected to tetragonal strain (20% in length) along the [100] direction. For TiN [Fig. 4(a)], the response to the strain along [100] consists primarily in a charge-density decrease along the same [100] direction, with no significant variations in charge density along the [010] direction. In other words, the strain along the [100] direction increases the ionic character of the Ti-N bond along this direction to an almost pure ionic interaction. A similar effect can be observed for TiAlN if one compares Figs. 3(b) and 4(b), case in which both Ti-N and Al-N bonds are mostly ionic along the strain direction. To some extent, the TiMoN response to tetragonal strain is similar [Fig. 4(c)] in the sense

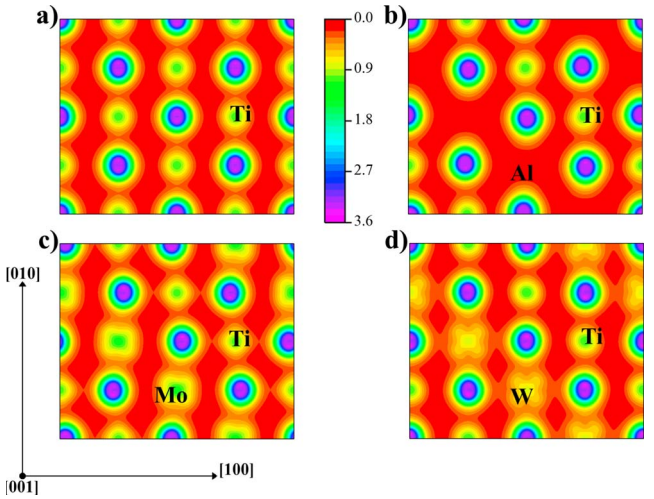

FIG. 4. (Color online) Charge densities of structures under tetragonal deformation (strain). Color scale units are electrons/Å^3: (a) TiN, (b) TiAlN, (c) TiMoN, and (d) TiWN.

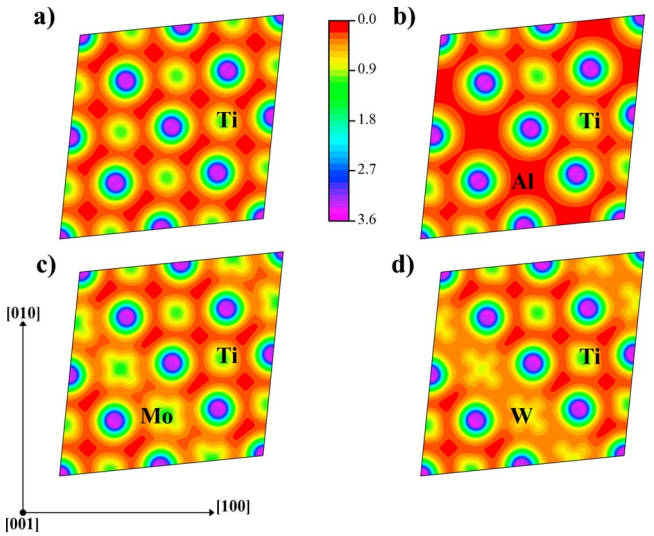

FIG. 5. (Color online) Charge densities of structures under trigonal deformation (shearing). Color scale units are electrons/Å^3: (a) TiN, (b) TiAlN, (c), TiMoN, and (d) TiWN.

that the Mo-N bond along [100] becomes mostly ionic. In this instance, however, the Ti-N bonds maintain significant covalent character along the strain direction, and to resist deformation and to preserve system stability, the lattice is distorted and loses its right angles. We do not observe equivalent structural changes for TiWN [Fig. 4(d)]. In this case, the Ti-N bonds become indeed ionic, but the W-N bonds maintain a high covalent character along the [100] strain direction as well as in the [010] direction and no lattice distortion is observed.

The response to shearing of each compound is shown in Fig. 5, where one can see the charge-density map of each structure subjected to a trigonal strain of 10% along the [110] direction. The comparison of Figs. 5(a) and 5(b) to Figs. 3(a) and 3(b) reveals that shearing does not introduce any change in the bonding character for TiN and TiAlN. The same mixture of ionic and covalent bondings, which is the signature of strong directional bonding, is present in both compounds. This is not, however, the situation for TiMoN and TiWN, where in response to shearing, the charge-density maps exhibit drastic changes [see Figs. 5(c), 5(d), 3(c), and 3(d)]. In both compounds, but particularly in TiWN, there is strong evidence of the formation of a layered electronic structure, consisting in alternating layers of high and low electrons concentration along the $[1\bar{1}0]$ direction, i.e., perpendicular to the direction of deformation. In the layers with high electron density, which follow the Mo-Mo or W-W stacking, bonding is obviously predominantly metallic, while in the layers with low electron density, which follow the Ti-Ti stacking, the ionic-covalent bonding type prevails. This electronic arrangement thus equates into alternating layers characterized by strong, angular-directional, respectively, weak bonding and is essential in explaining the dual hard-ductile nature of these ternaries.

We note that analogous arrangements of electrons, in layered structures, have been used to explain the high bulk moduli and low C_{44} constants reported for a number of MAX

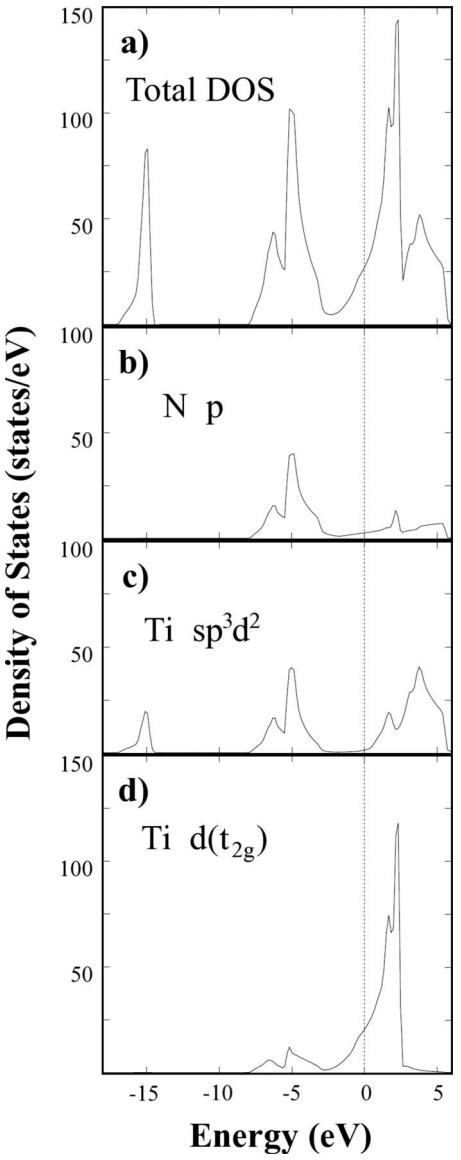

FIG. 6. Partial and total density of states for TiN.

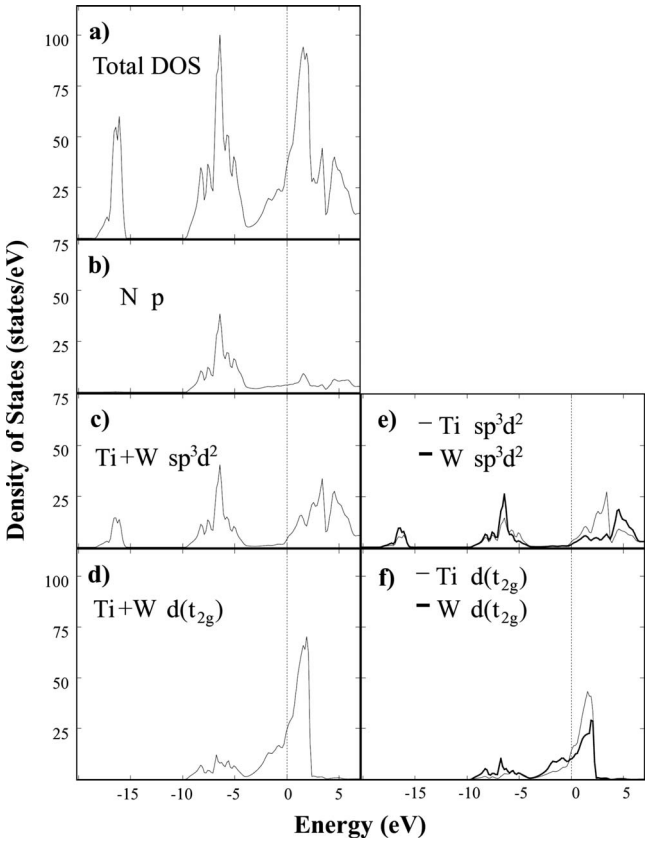

FIG. 7. Partial and total density of states for TiWN.

phases and nanolaminates[40] and connected to the malleability of these materials. The difference is that the electronic layered structure reported herein is induced by the deformation, compared to the *de facto,* existing layering of electrons in MAX phases. At this point in discussion, one should emphasize that a very clear feature of the charge-density maps shown in Figs. 3(c) and 3(d) is the spreading toward second-nearest neighbors of the charge surrounding Mo and W atoms, i.e., along the Mo-Mo, respectively, W-W, stacking. This is indeed the precursor, the origin, of the alternate metallic/ionic-covalent bonding in these ternaries, the layered electronic structure induced during deformation.

These arguments are supported by our DOS results, for the TiN and TiWN relaxed structures, which are shown in Fig. 6, respectively, in Fig. 7. For TiN, one can observe, Figs. 6(b) and 6(c), a strong hybridization due to the $p(\mathrm{N})-sp^3d^2(\mathrm{Ti})$ orbital overlapping. The corresponding populated σ bonding states are indicated by the peaks in the $[-8,-3\ \mathrm{eV}]$ energy interval, separated by a gap of ~ 3 eV from the unpopulated σ^* antibonding states, located just above the Fermi level. Similarly, in Figs. 7(b) and 7(c), for TiWN, one can see the occupied σ bonding states in the $[-10,-4\ \mathrm{eV}]$ interval, due to the Ti-N and W-N first neighbor interactions, separated from the unoccupied σ^* antibonding states by a gap of ~ 4 eV. The DOS of the two compounds differ in the occupation of the states derived from the $d(t_{2g})$ orbitals [Fig. 6(d) and 7(d)]. The reason is that the ternaries, by comparison to TiN, have one more valence electron per unit cell and the d-t_{2g} orbitals of each Mo-Mo or W-W pair of atoms come close to overlapping and enable better filling of the t_{2g} bands. The spreading of the charge in the vicinity of Mo or W atoms [Fig. 3(c) and 3(d)] and the partial DOS plots for the W t_{2g}-t_{2g} states in Fig. 7(f) clearly support these arguments. During any shearing deformation, this situation is favored even more so, as the second neighbors distance gets shorter, the d-t_{2g} Mo or W orbitals start to overlap, and the metal-metal interaction is strengthened. This is the mechanism responsible for the layered electronic structure and for inducing the metallic bonding observed in these ternaries. Significantly, we note that this type of $d(t_{2g})$-$d(t_{2g})$ orbitals was also shown to be sensitive to shear deformations in MAX phase M_2AlN nitrides[41] and M_2AlC carbides,[42] as well as in carbonitrides.[43]

IV. CONCLUSION

We use *ab initio* calculations to accurately estimate the effects of alloying TiN with two transition metals, Mo and

W, in concentrations of 50%. The results show that these ternaries retain similar hardness to that of TiN and $Ti_{0.5}Al_{0.5}N$ and have a significantly increased ductile behavior, i.e., enhanced toughness compared to the pure binary or ternary. We investigate the electronic structure of these ternaries and examine the changes induced by the additional transition metals in the distribution of the electronic charge. This analysis reveals that the mechanism responsible for toughness enhancement is the formation of a layered electronic structure, primarily by metallic $d(t_{2g})$-$d(t_{2g})$ orbitals, which allow a selective response of the B1 structure to strain and shear deformations.

ACKNOWLEDGMENT

All calculations were performed on the Neolith cluster located at the National Supercomputer Centre (NSC) in Linköping.

[1] P. H. Mayrhofer, C. Mitterer, L. Hultman, and H. Clemens, Prog. Mater. Sci. **51**, 1032 (2006).
[2] P. H. Mayrhofer, A. Hörling, L. Karlsson, J. Sjölen, T. Larsson, C. Mitterer, and L. Hultman, Appl. Phys. Lett. **83**, 2049 (2003).
[3] A. Hörling, L. Hultman, M. Oden, J. Sjölen, and L. Karlsson, Surf. Coat. Technol. **191**, 384 (2005).
[4] M. Moser and P. H. Mayrhofer, Scr. Mater. **57**, 357 (2007).
[5] J. Zhang, W. Y. Guo, Y. Zhang, Q. Guo, C. Wang, and L. P. Zhang, Thin Solid Films **517**, 4830 (2009).
[6] P. L. Tam, Z. F. Zhou, P. W. Shum, and K. Y. Li, Thin Solid Films **516**, 5725 (2008).
[7] K. Yamamoto, T. Sato, K. Takahara, and K. Hanaguri, Surf. Coat. Technol. **174-175**, 620 (2003).
[8] C. Feng, S. Zhu, M. Li, L. Xin, and F. Wang, Surf. Coat. Technol. **202**, 3257 (2008).
[9] M. Pfeiler, K. Kutschej, M. Penoy, C. Michotte, C. Mitterer, and M. Kathrein, Surf. Coat. Technol. **202**, 1050 (2007).
[10] A. E. Santana, A. Karimi, V. H. Derflinger, and A. Schutze, Mater. Sci. Eng., A **406**, 11 (2005).
[11] S. F. Pugh, Philos. Mag. **45**, 823 (1954).
[12] D. G. Pettifor, Mater. Sci. Technol. **8**, 345 (1992).
[13] J. Haines, J. M. Leger, and G. Bocquillon, Annu. Rev. Mater. Res. **31**, 1 (2001).
[14] K. Y. Chen, L. R. Zhao, J. Rodgers, and J. S. Tse, J. Phys. D **36**, 2725 (2003).
[15] L. R. Zhao, K. Chen, Q. Yang, J. R. Rodgers, and S. H. Chiou, Surf. Coat. Technol. **200**, 1595 (2005).
[16] H. W. Hugosson, U. Jansson, B. Johansson, and O. Eriksson, Science **293**, 2434 (2001).
[17] T. Joelsson, L. Hultman, H. W. Hugosson, and J. M. Molina-Aldareguia, Appl. Phys. Lett. **86**, 131922 (2005).
[18] J. H. Moser, F. Tian, O. Haller, D. B. Bergstrom, I. Petrov, J. E. Greene, and C. Wiemer, Thin Solid Films **253**, 445 (1994).
[19] F. Tian, J. D'Arcy-Gall, T. Y. Lee, M. Sardela, D. Gall, I. Petrov, and J. E. Greene, J. Vac. Sci. Technol. A **21**, 140 (2003).
[20] R. Sanjines, C. Wiemer, J. Almeida, and F. Levy, Thin Solid Films **290-291**, 334 (1996).
[21] Q. Yang, L. R. Zhao, P. C. Patnaik, and X. T. Zeng, Wear **261**, 119 (2006).
[22] G. Kresse and J. Hafner, Phys. Rev. B **49**, 14251 (1994).
[23] J. P. Perdew and Y. Wang, Phys. Rev. B **45**, 13244 (1992).
[24] P. E. Blöchl, Phys. Rev. B **50**, 17953 (1994).
[25] H. J. Monkhorst and J. D. Pack, Phys. Rev. B **13**, 5188 (1976).
[26] B. Alling, A. V. Ruban, A. Karimi, O. E. Peil, S. I. Simak, L. Hultman, and I. A. Abrikosov, Phys. Rev. B **75**, 045123 (2007).
[27] P. H. Mayrhofer, D. Music, and J. M. Schneider, J. Appl. Phys. **100**, 094906 (2006).
[28] F. Birch, J. Geophys. Res. **83**, 1257 (1978).
[29] J. O. Kim, J. D. Achenbach, P. B. Mirkarimi, M. Shinn, and S. A. Barnett, J. Appl. Phys. **72**, 1805 (1992).
[30] A. Hoerling, J. Sjölen, H. Willmann, T. Larsson, M. Oden, and L. Hultman, Thin Solid Films **516**, 6421 (2008).
[31] T. Lee, K. Ohmori, C. S. Shin, D. G. Cahill, I. Petrov, and J. E. Greene, Phys. Rev. B **71**, 144106 (2005).
[32] C. Sarioglu, Surf. Coat. Technol. **201**, 707 (2006).
[33] L. Marques, S. Carvalho, F. Vaz, M. M. D. Ramos, and L. Rebouta, Vacuum **83**, 1240 (2009).
[34] S. Nagao, K. Nordlund, and R. Nowak, Phys. Rev. B **73**, 144113 (2006).
[35] R. Ahuja, O. Eriksson, J. M. Wills, and B. Johansson, Phys. Rev. B **53**, 3072 (1996).
[36] S. H. N. Lim, D. G. McCulloch, M. M. M. Bilek, D. R. McKenzie, S. P. Russo, A. S. Barnard, and A. Torpy, J. Phys.: Condens. Matter **17**, 2791 (2005).
[37] V. Podgursky, J. Phys. D **40**, 4021 (2007).
[38] M. Ahlgren and H. Blomqvist, Surf. Coat. Technol. **200**, 157 (2005).
[39] A. Kimura, M. Kawate, H. Hasegawa, and T. Suzuki, Surf. Coat. Technol. **169-170**, 367 (2003).
[40] D. Music and J. M. Schneider, JOM **59**, 60 (2007).
[41] Z. M. Sun, D. Music, R. Ahuja, and J. M. Schneider, Phys. Rev. B **71**, 193402 (2005).
[42] J. Emmerlich, D. Music, A. Houben, R. Dronskowski, and J. M. Schneider, Phys. Rev. B **76**, 224111 (2007).
[43] S. H. Jhi, J. Ihm, S. G. Louie, and M. L. Cohen, Nature (London) **399**, 132 (1999).